Nat. Hazards Earth Syst. Sci. Discuss., 2, 1433–1464, 2014
www.nat-hazards-earth-syst-sci-discuss.net/2/1433/2014/
doi:10.5194/nhessd-2-1433-2014

Natural Hazards and Earth System Sciences
Open Access
Discussions

Numerical modeling and analysis of the effect of Greek complex topography on tornado genesis

I. T. Matsangouras[1], I. Pytharoulis[2], and P. T. Nastos[1]

[1]Laboratory of Climatology and Atmospheric Environment, Faculty of Geology and Geoenvironment, University of Athens, Panepistimioupolis 15784, Athens, Greece
[2]Department of Meteorology and Climatology, School of Geology, Aristotle University of Thessaloniki, University Campus 54124, Thessaloniki, Greece

Received: 16 January 2014 – Accepted: 20 January 2014 – Published: 11 February 2014

Correspondence to: I. T. Matsangouras (john_matsa@geol.uoa.gr)

Published by Copernicus Publications on behalf of the European Geosciences Union.

Abstract

Tornadoes have been reported in Greece over the last decades in specific sub-geographical areas and have been associated with strong synoptic forcing. It is well known that meteorological conditions over Greece are affected at various scales by the significant variability of topography, the Ionian Sea at the west and the Aegean Sea at the east. However, there is still uncertainty regarding topography's importance on tornadic generation and development.

The aim of this study is to investigate the role of topography in significant tornado genesis events that were triggered under strong synoptic scale forcing over Greece. Three tornado events that occurred over the last years in Thiva (Boeotia, 17 November 2007), Vrastema (Chalkidiki, 12 February 2010) and Vlychos (Lefkada, 20 September 2011) have been selected for numerical experiments. These events were associated with synoptic scale forcing, while their intensity was T4–T5 (Torro scale) and caused significant damage. The simulations were performed using the non-hydrostatic Weather Research and Forecasting model (WRF), initialized with ECMWF gridded analyses, with telescoping nested grids that allow the representation of atmospheric circulations ranging from the synoptic scale down to the meso scale. In the experiments the topography of the inner grid was modified by: (a) 0 % (actual topography) and (b) −100 % (without topography). The aim was to determine whether the occurrence of tornadoes – mainly identified by various severe weather instability indices – could be indicated by modifying topography. The main utilized instability variables concerned the Bulk Richardson number shear (BRN), the energy helicity index (EHI), the storm-relative environmental helicity (SRH) and the maximum convective available potential energy (MCAPE, for parcel with maximum theta-e). Additional a verification of model was conducted for every sensitivity experiment accompanied with analysis absolute vorticity budget.

Numerical simulations revealed that the complex topography was denoted as an important factor during 17 November 2007 and 12 February 2010 events, based on EHI

and BRN analyses. Topography around 20 September 2011 event was characterized as the least factor based on EHI, SRH, BRN analyses.

1 Introduction

Tornadoes are violently rotating columns of air, associated with swirling cloud of debris and a funnel shaped cloud extending downward from the base of the parent cumulonimbus cloud. They are associated with extremely high winds, inside and around the tornado's funnel, causing extended damage and in many cases loss of life. Tornadoes and waterspouts have always fascinating to mankind; were well known to the ancients; virtually all of the classical philosophers have provided possible explanations of them and during the last 40 yr researchers have motivated studies and attempts to understand the mechanisms that produced these phenomena.

Climatological studies described the spatio-temporal distribution of tornadoes, revealing that they are not a rare and unknown phenomenon in Greece (Nastos and Matsangouras 2010; Matsangouras et al., 2011b, 2013; Sioutas, 2011). In addition to these climatological research works, reports and case studies of some important tornado and waterspout events that occurred in Greece have been carried out (Matsangouras and Nastos 2010; Matsangouras et al., 2010, 2011a, 2012; Nastos and Matsangouras 2012; Sioutas et al., 2012).

Tornadogenesis is a major forecast challenge in regions of complex terrain (e.g., Homar et al., 2003) and Greek's complex inland terrain along with the Ionian Sea at the west and the Aegean Sea at the east, appears to be a vulnerable area for convective weather and tornado occurrence. Operational and research meteorologists often refer and investigate the presence of diagnostic variable set that can be used as forecast parameters for severe convective weather. Diagnostic variables have a long history in association with forecasting severe convective weather (Schaefer 1986; Johns and Doswell, 1992) as their values represent its capacity to summarize in a single value some kinematic or thermodynamics characteristics of the severe storm environment.

NHESSD

2, 1433–1464, 2014

Doswell and Schultz (2006) discussed clearly these diagnostic variables and introduced a classification scheme about them: (1) *simple observed variables*, (2) *simple calculated variables*, (3) *derivatives or integrals (spatial or temporal) of simple observed or calculated variables*, (4) *combined variables* and (5) *indices*. Do these diagnostic variables are sufficient to forecast tornadogenesis? What other factors made the environment conditions favourable for tornadoes?

In order to answer these questions we need to review which diagnostic variables have been identified by prior research as "ingredients" for tornado occurrence. The concept of ingredients was introduced by Doswell (1987), Doswell et al. (1996) and Groenemeijer et al. (2011), and can be characterized as a necessary, but not sufficient, requisite for a phenomenon to occur. Firstly, the storm itself requires two ingredients: (1) Convective Available Potential Energy (CAPE; Table 1) and (2) lift. By lift we mean the sufficient initial vertical motion to result in convection and this could be carried out by thermal process, by a synoptic driven force (fronts) or by the effect of topography-orography. Miglietta and Regano (2008) confirmed the importance of the orography for the development of convective cells, using WRF sensitivity experiment over a small area in Apulia (in southern Italy). Regarding CAPE, several researchers have noted that large values of CAPE are not mandatory for tornado development (Monteverdi et al., 2003; Hannesen et al., 1998; Groenemeijer and Van Delden, 2007). Besides CAPE, Rasmussen (2003) has shown that the storm relative helicity (SRH) in the lowest atmosphere (Table 1) can be used to distinguish non-tornadic, weakly and significantly tornadic storms. Craven and Brooks (2002) and Brooks (2009), noted that the strong low level wind shear has been identified as a good predictor for tornadoes. Energy helicity index (EHI; Table 1) was evaluated by Rasmussen (2003) based on three classes of proximity soundings relating convective weather and super-cells storms with tornadic and non tornadic events. The Bulk Richardson Number (BRN, Table 1) is used to quantify the relationship between buoyant energy and vertical wind shear (Moncrieff and Green, 1972), taking into account the wind components of the difference between the density-weighted mean winds over the lowest 6000 m and the lowest 500 m a.g.l.

As discussed in Droegemeier et al. (1993), the BRN is only a gross estimate of the effects of vertical wind shear on convective storms, since it does not measure the turning of the wind profile with height. However, Weisman and Klemp (1984) show using cloud-scale model simulations that the BRN can distinguish between supercell and multicell storms, with modeled supercells likely when $10 \leq \text{BRN} \leq 50$ and multicells storms likely when $\text{BRN} > 35$. It is important to note that there is no well-defined threshold value for BRN, since there is an overlap in these values used to specify storm type.

A model simulation with spatial resolution that reproduces the weather conditions at storm scale is a powerful tool for understanding the relevant physical processes involved and calculate the aforementioned diagnostic variables. In our study 3 tornado events were simulated using the non-hydrostatic Weather Research and Forecasting (WRF) model, in order to determine whether the model is able to indicate the occurrence of tornadic activity by modifying the topography. The selected tornado events were associated with synoptic scale forcing; their intensity was T4–T5 of TORRO scale (Meaden, 1976) and caused significant damages. These tornado events occurred over Greece during the last years in Thiva (Boeotia, 17 November 2007), Vrastema (Chalkidiki, 12 February 2010) and Vlychos (Lefkada, 20 September 2011).

An analysis of severe weather variables was conducted for every simulation. These diagnostic variables concern the Bulk Richardson number shear (BRN), the energy helicity index (EHI), the storm-relative environmental helicity (SRH) and maximum convective available potential energy (MCAPE, for parcel with maximum theta-e). The low-level SRH, can vary dramatically over short distances, due to topographically-channelled flow (e.g., Braun and Monteverdi, 1991; Bosart et al., 2006). The selection of these parameters is consistent with the approach adopted in previous studies (Droegemeier et al., 1993; Johns et al., 1993; Rasmussen and Blanchard, 1998; Brooks et al., 2003; Doswell and Evans, 2003; Thompson et al., 2003; Shafer et al., 2009; Matsangouras et al., 2011a, 2012).

The purpose of this paper is to investigate the importance of complex terrain in tornadoes formation. The data sources and WRF setup are presented in Sect. 2. Section 3

NHESSD
2, 1433–1464, 2014

analyzes the tornado events and a briefly weather synoptic analyses is presented, while in Sect. 4 we present the model simulation verification. In Sect. 5 we present the analysis of absolute vorticity budget and in Sect. 6 we analyze and discuss our results, while Sect. 7 summarizes our results and conclusions.

2 Data sources and model setup

The Laboratory of Climatology and Atmospheric Environment (LACAE, http://lacae.geol.uoa.gr) at University of Athens has undertaken a systematic effort in recording tornadoes, waterspouts, and funnel clouds in Greece beginning in 2007. LACAE developed in 2009 an open-ended online tornado report database web system (http://tornado.geol.uoa.gr), contributing to the compilation of a climatology of these extreme weather events. A flow chart of the LACAE tornado report data stream system accompanied with the plausibility check process is presented by Matsangouras et al. (2013). LACAE is in close collaboration with European Severe Storm Laboratory (ESSL) and submits on a regular basis its report to European Severe Weather Database (ESWD).

The three tornado cases: (1) Thiva (Boeotia, 17 November 2007), (2) Vrastema (Chalkidiki, 12 February 2010) and (3) Vlychos (Lefkada, 20 September 2011) were reported to LACAE's tornado database. The selected tornado events were associated with synoptic scale forcing (frontal activity), their intensity was T4–T5 of TORRO scale and caused significant damages.

Tornadoes event simulations were performed using the non-hydrostatic Weather Research and Forecasting (WRF) model with the dynamical core of Advanced Research WRF (WRF-ARW). An analysis of BRN, EHI, SRH and maximum convective available potential energy (MCAPE, for parcel with maximum theta-e) severe weather variables were conducted for every simulation.

The WRF-ARW V3.2 non-hydrostatic numerical model (Skamarock et al., 2008; Wang et al., 2010) was used in order to simulate the weather conditions regarding tornadic activity on 17 November 2007, 12 February 2010 and 20 September 2011. Three one-way nested domains were utilised. The spatial resolution of the model was 12 km for D1 (381 × 301 grid-points), 4 km for D2 (310 × 301 grid-points) and 1.333 km for D3 (202 × 202 grid-points). Figure 1 illustrates all nested domains for every case study. All nests were integrated in non-hydrostatic mode. In all cases domain D1 covered Europe and northern Africa and D2 covered an area from southern Balkans (northern boundaries) to the north coasts of Africa (southern boundaries), and from south Italy to east Turkey. D3 was setup over each area of interest. In the sensitivity experiments, topography was modified only in D3 domain. Figure 1 illustrates the actual topography of Greece and the three nested domains. In the vertical, 39 sigma levels (up to 50 hPa) with increased resolution in the boundary layer were used by all nests. ERA-Interim reanalyses (Dee et al., 2011) from European Centre for Medium-Range Weather Forecasts (ECMWF) with a spatial resolution of $0.75^{\circ} \times 0.75^{\circ}$ were used as initial and lateral boundary conditions for the domain D1. The selection of the aforementioned datasets was made for homogenization purposes of initial and boundaries conditions for all cases. The upper air fields were available at 1000, 925, 850, 700, 500, 400, 300, 250, 200, 150, 100, 70, 50 hPa. The sea-surface temperatures (SSTs) were derived from the daily National Centers of Environmental Prediction (NCEP) SST files at a very high horizontal resolution of $0.083^{\circ} \times 0.083^{\circ}$.

The Ferrier (Ferrier et al., 2002), RRTMG scheme (Iacono et al., 2008), the Monin–Obukhov (Eta) (Janjic, 1996) and the Mellor–Yamada–Janjic (Mellor and Yamada, 1982; Janjic, 2002) level 2.5 scheme were used in all nests to represent microphysics, longwave/shortwave radiation, surface layer and boundary layer, respectively. The soil processes are represented by the NOAH Unified model (Chen and Dudhia, 2001) in 4 layers (0–10 cm, 10–40 cm, 40–100 cm, 100–200 cm). Cumulus convection was parameterized only in nests D1 and D2 by the most recent version of the Kain–Fritsch scheme (Kain, 2004).

The model was initialised at 00:00 UTC, on 17 November 2007 (∼ 23 h before the event) for 2007 tornado even. For the tornado events of 2010 and 2011, the model

NHESSD
2, 1433–1464, 2014

was initialized at 00:00 UTC on 12 February 2010 (∼ 16 h before the event) and at 00:00 UTC on 20 September 2011 (∼ 13 h before the event), respectively. The time of initialization was selected in order to examine the model's forecast ability of more than 12 forecast hours ahead to depict any significant value of previous diagnostic variables.

The model outputs were available at 10 min interval. This interval was chosen to investigate the ability of the WRF to simulate in short time intervals the evolution of convective weather events, providing qualitative and quantitative evidence as to the degree of synoptic scale involvement, influenced by topography modifications.

3 Tornadic events and synoptic analyses

In this section a briefly tornado and synoptic analyses for every tornado events is presented. Synoptic analyses concern the pressure level of 500 hPa, based on ECMWF ERA-Interim analysis archive dataset, and the mean sea level (MSL) pressure based on UK Met Office (UKMO) MSL pressure analyses. Figure 2 illustrates a collection of images revealing the force, the impact and damage caused by every tornado to the local society. Hereafter, for brevity reasons, we coded the tornadoes as TXX, where T stands for tornado and XX represent the last two digits of the year that tornado occurred (e.g. T10 = Tornado event that occurred in 2010).

The first tornado event (hereafter T07) formed approximately (±5 min) at 21:20 UTC on 17 November 2007, over Loutoufi, a small village located 9 km SW of Thiva's city (Lat: 38.28° N, Lon: 23.28° E; Fig. 1). The tornado dissipated at Thiva's NW urban area (Piri district), its path was 10 km and scattered broken branches of olive trees were found along it (Fig. 2a and b). Additionally, significant damages were documented in Loutoufi village and in Thiva city (structural damages). Regarding tornado's force scale it could be characterized as a T4–T5 of TORRO scale, based on tornado's damage survey. Synoptic analysis at the isobaric level at 18:00 UTC of 500 hPa (not shown), depicts a closed cyclonic circulation over central Italy, implying a SW upper air stream over west Greece. A long through line is positioned from south parts of Italy to the northern parts of Libyan, accompanied by a thermal through of −20 °C. UKMOs MSL pressure analysis at 18:00 UTC (Fig. 3a) illustrates a cold front activity over west Greece.

The third tornado (hereafter as T10) occurred 2.5 km south of Chalkidiki's Vrastama village, a non urban area 45 km southeast of Thessaloniki in northern Greece (Lat: 40.36, Lon: 23.54; Fig. 1), on 12 February 2010. The T10 developed approximately between 17:10 and 17:35 UTC, it caused significant damage to a green-olive processing unit and to several olive oil farms (more than 100 olive trees were uprooted). Based on the caused damage (Fig. 2c and d), it could be characterized as T4–T5 of TORRO scale. ECMWF's ERA-Interim upper air analyses at the isobaric level of 500 hPa (not shown), during the day of T10 event, showed a closed cyclonic circulation associated with cold air masses (−35 °C), inducing a SW upper air flow over the area of interest at 12:00 UTC. The cylonic circulation extended throughout the lower troposphere, UKMO's MSL pressure analyses at 18:00 UTC (Fig. 3b) showed a cold front extended from northern Greece to Peloponnesus (south Greece) and northern Libya.

The last tornado event (hereafter as T11) developed approximately (±10 min) at 15:20 UTC time, on 20 September 2011, over Vlychos (Lat: 38.68° N, Lon: 20.69° E; Fig. 1), a small village at the island of Lefkada, over west Greece. T11 caused significant damage at Vlycho's marina (Fig. 2e and f) and 1 casualty was recorded, tornado's intensity was also categorized as T4–T5 TORRO scale. At 500 hPa (not shown) a closed cyclonic circulation over central Italy accompanied with a long wave trough along south parts of Italy, caused a SW upper air stream over west Greece. MSL pressure analysis at 12:00 UTC illustrates frontal wave activity along west coasts of Greece (Fig. 3c).

A detailed synoptic analysis accompanied with remote sensing data (satellite and radar images) for T10 event was presented by Matsangouras et al. (2011a). The synoptic weather conditions and analysis during T07 tornado event day were also discussed by Matsangouras et al. (2012). Visualizations of weather conditions (spatial distribution of lightning activity and ground observations) for T10 and T11 events are presented in Fig. 4, based on Hellenic National Meteorological Service (HNMS) archive dataset.

Images were produced via HNMS's METshell software (version v.2010.a) tailored for operational forecasting usage (Basiakos et al., 2000).

4 Model verification

The analysis of the model errors in the control simulations on the day of each tornado event is presented in Table 2. The statistics are calculated using the available METAR observations and the corresponding model values of the innermost domain (D03) at the locations of the meteorological stations of the HMMS that are nearest to each tornado event. Figure 1 illustrates the location of tornadoes and meteorological stations (blue and red abbreviations). The distance of these stations from the corresponding tornado events ranged from 26 km to 65 km and they are considered representative of the meteorological conditions in the ambient environment of the tornadoes. Statistical measures of 10 m wind speed (WS), temperature (T), dew point temperature (Td) and mean sea-level pressure (MSLP) at the meteorological stations are presented in Table 2.

The model overestimated the 10 m wind speed at all stations from 0.79 to 2.08 m s^{-1}. The MAE and RMSE of the 10 m wind speed ranged from 1.78 to 3.32 m s^{-1} and from 2.33 to 4.05 m s^{-1}, respectively. The 2 m temperature and the 2 m dew-point temperature were overestimated in all control simulations. The MAE (RMSE) of temperature was between 1.38 K (1.95 K) and 1.94 K (2.21 K), reaching 4.41 K (5.28 K) at LGTG (case of 17 November 2007). The dew-point temperature MAE and RMSE ranged from 1.57 to 3.35 K and from 1.57 to 4 K, respectively. Finally, the bias of the mean sea-level pressure was either close to 0 or negative and its values ranged from 0.33 to −1.25 hPa. Its MAE was between 1.2 and 2.05 hPa, while the range of the RMSE was from 1.4 to 2.26 hPa.

The abovementioned scores are in general agreement with statistical evaluations of modern high resolution numerical weather prediction models in Greece. Gofa et al. (2008) validated the operational HNMS forecasts of SKIRON (0.06° × 0.06°) and

COSMO-GR (0.0625° × 0.0625°) models for 2007 and found RMSE between: (a) 2.2 and 2.5 $m\,s^{-1}$ for the 10 m wind speed, (b) 1.9 and 2.6 K for 2 m temperature, (c) 2.3 and 3.5 K for 2 m dew-point temperature and (d) 1 and 2 hPa for the mean sea-level pressure, in the first 1–2 forecast days. Pytharoulis (2009) evaluated SKIRON model (0.05° × 0.05°) in Greece for the period June 2007–April 2009. During the first forecast days, the latter model exhibited RMSE between: (a) 2.2 and 2.7 $m\,s^{-1}$ for the 10 m wind speed, (b) 2 and 2.5 K for 2 m temperature and (c) 1 and 1.5 hPa for the mean sea-level pressure. Papadopoulos and Katsafados (2009) evaluated POSEIDON forecasting system (0.05° × 0.05°) across the eastern Mediterranean from mid-November 2007 to October 2008 and obtained RMSE between: (a) 2.4 and 2.7 $m\,s^{-1}$ for the 10 m wind speed, (b) 2.3 and 2.9 K for the 2 m temperature and (c) 1.2 and 1.8 hPa for the mean sea-level pressure, in the first 2 forecast days.

In this study the model errors are generally within the values that appear in the literature, with a few exceptions (e.g. the 2 m temperature at LGTS, the 2 m dew-point temperature at LGPZ). The only parameter that systematically exhibited high values of RMSE is the 10 m wind speed. Some possible reasons for these errors are:

(a) They correspond to high-impact weather events at individual stations and not to different weather types for multiple stations and long periods. In this study most of the stations were under the influence of cumulonimbus activity for several hours. Even if a numerical model is successful in representing convective activity, it is very difficult to represent adequately the mesoscale flow induced by the storm. Ebert (2008) argues that although high-resolution numerical weather predictions can look quite realistic and be very useful, they have a "difficulty of predicting an exact match to the observations".

(b) The model values were extracted from domain 3 that is integrated with a timestep of 8 s. On the contrary, the observed 10 m wind speeds are 10 min average values.

(c) The evaluation is based on METAR and not on SYNOP observations, introducing a maximum error up to +0.33 hPa in mean sea-level pressure and ±0.5 K in 2 m

NHESSD
2, 1433–1464, 2014

temperature and 2 m dew-point temperature. Moreover, the fact that the METARs are available in hourly or half-hourly intervals (contrary to the other studies that are based on 6 hourly SYNOP) forces the calculated errors to take into account even temporary model miscalculations.

5 Absolute vorticity budget

The vorticity field and the vorticity equation are useful tools, commonly employed in studies of atmospheric dynamics. The absolute vorticity and the vorticity equation terms were derived at 10 min intervals at a height of 1 km above sea-level. This height was selected because in the nature it is generally located near the base of thunderstorms and in the simulations it was found above the model topography (at the location of each actual tornado). The values of the above terms, but not the conclusions, were modified when the height was moderately increased (up to 2 km). The calculations were performed using the Grid Analysis and Display System (GrADS) and were based on the simulated WRF parameters of the innermost domain (D3). The necessary upper air fields were vertically interpolated at 250 m intervals before the calculation of the vertical derivatives. All the derivatives were estimated using second order centered finite differences.

Figures 5–7 illustrate timeseries of the maximum values of the absolute vorticity and of the vorticity equation terms of horizontal and vertical advection, tilting/twisting and divergence in a box of $0.2^{\circ} \times 0.2^{\circ}$ latitude-longitude centered at the actual location of each tornado. It was chosen to exhibit the results in a limited area and not locally, in order to consider any shift of the meteorological conditions due to model error. Both experiments (with and without topography) are shown for each tornado case. The solenoidal term is not displayed because it was computed to be at least four orders of magnitude lower than the other terms. A very limited number of grid-points with topography above or equal to 1 km within the abovementioned area (of $0.2^{\circ} \times 0.2^{\circ}$) were not taken into account.

NHESSD
2, 1433–1464, 2014

Effect of Greek complex topography on tornado genesis

I. T. Matsangouras et al.

The most important term of the vorticity equation appears to be the horizontal advection, with maximum values up to 0.35 (0.29) $s^{-1}\,hr^{-1}$ in the case of 12 February 2010 with (without) topography. The predominance of this term in these case studies is likely to be associated with the prevailing strong synoptic forcing due to the cold front. The vertical advection and twisting/tilting of horizontal vorticity to the vertical direction appear to be similarly important without significant differences, while the divergence term has generally a smaller contribution than the previous two terms. In real supercells the tilting of horizontal vorticity generated along the gust front into the vertical is a significant source of low-level vorticity (Houze, 1993). However, this mechanism cannot be adequately represented in the simulations of this article, despite their fine grid spacing (1.333 km × 1.333 km in D3).

In all cases the simulations with topography are associated with higher values of maximum absolute vorticity in the area of interest than those without topography (Figs. 5–7). Similarly, the vorticity equation terms that determine the Eulerian time change of vorticity display higher maximum values in the experiment with topography. The differences between the two experiments, and the concomitant importance of topography for tornado genesis, are more distinguishable in the cases of 17 November 2007 (Fig. 5) and 12 February 2010 (Fig. 6). The former tornado occurred at a location surrounded by mountains and the latter one developed at the mountains of Chalkidiki, Northern Greece.

6 Results and discussion

In this section we present the results of numerical simulations analyses of EHI, BRN, SRH and MCAPE diagnostic variables based on the actually topography and modified topography at the inner domain box (D3 as described at Sect. 2). The actual topography is illustrated in Fig. 1a, in meters. Hereafter, for brevity reasons, the numerical simulations results based on modified (reducing) topography of D3 domain will be coded as TOPOMX, where X stands the percentage (%) of modification (reducing). Thus, TOPOM0 means modified topography by 0 % (actual topography), and TOPOM100 was coded as the modified topography by −100 % (without topography). In all cases, variables' discussion and analysis concern a period time of 2 h prior to tornado formation and ending 1 h after that.

At T07 TOPOM0 simulation, EHI analysis an area of high values (> 5) was located 40 km S-SW from Thiva (over the Gulf of Korinthos). With time evolution that area was expanded over the area of tornado and 30 min before the tornado formations a value of 8 was recorded. SRH variable revealed a high value of more than 1000 $m^2 s^{-2}$ 40 km S-SW from Thiva (over the Gulf of Korinthos). Around the time of tornado development, values of SRH over the area of study were more than 1400 $m^2 s^{-2}$. BRN variable experienced the maximum value of 800 $m^2 s^{-2}$ S-SW from Thiva. Over that high values of BRN remained constantly high. MCAPE's variable spatial and temporal distribution was similar with the others variable behaviour (maximum values 40 km S from Thiva). Around the T07 formation an expansion of high values were recorded near Thiva. Regarding T07's TOPOM100 simulation, EHI depicted an area of EHI values less than 4, 40 km S of tornado location. With time evaluation it was propagated eastwards and around the time of formation the values are less than 2. Similarly the SRH variable was depicted over the Gulf of Korinthos area, with values less than 1000 $m^2 s^{-2}$, and no significant change was recorder over the area of interest later. BRN variable revealed values of 600 $m^2 s^{-2}$ over Corinthians' Gulf and were fast propagated eastwards compare with values from TOPOM0 simulation. Similarly with the BRN, SRH and EHI variable behaviour, MCAPE variable was higher (1000 $J kg^{-2}$) over southern parts, propagating very fast (compare with TOPOM0 simulation) over east parts.

Studing the simulation results of T10 TOPOM0 and TOPOM100, EHI maximum values were illustrated over the southern parts of Chalkidiki propagating to NE. Over the area of interest EHI's values based on TOPOM0 and TOPOM100 experiments did not illustrate any significant difference (the difference was less than 1 EHI value). Regarding SRH analyses, in both simulation (TOPOM0 and TOPOM100), over the Gulf of Thermaikos (the gulf west of Chalkidiki) an area of maximum values were depicted

NHESSD
2, 1433–1464, 2014

(more than 1800 $m^2 s^{-2}$ at TOPOM0 and more than 1200 $m^2 s^{-2}$ at TOPOM100) propagating eastwards. Around the time of T10 development SRH's values over tornado's location were increased to 2200 and 1600 $m^2 s^{-2}$ respectively. BRN variable during TOPOM0 and TOPOM100 did not present any significant change as it was varying from 100 to 200 $m^2 s^{-2}$. Around the T10 formation time, the BRN variable in both simulations, was increased to 400 $m^2 s^{-2}$. MCAPE analyses revealed an area of maximum MCAPE positioned over the south parts of Chalkidiki propagating NE, at TOPOM0 and TOPOM100 simulations. MCAPE values did not show any significant variations at TOPOM0 and TOPOM100 experiments, as they both captured a value of 1200 $J Kg^{-2}$, approximately at time of T10 formation.

Regarding T11 TOPOM0 simulations EHI, SRH and BRN analyses illustrated an area of high values, associated with the storm, propagating eastwards. A maximum value of 1800 $J Kg^{-2}$ was recorded over the area from MCAPE analyses. Compare with TOPOM0, TOPOM100 experiment the EHI, SRH and BRN variable did not reveal any significant variance over the area of interest.

Figure 8 summarizes the aforementioned analyses per diagnostic variable. Graphics illustrating the difference of TOPOM100 from TOPOM0 simulations (TOPOM0-TOPOM100) per diagnostic variable for every tornadic case study. Positive values implying a positive impact of topography, values equal to 0 no impact of topography and negative values negative impact of topography to diagnostic variables. The time axis analyses concern a time window from 90 min prior of tornado to 60 min after that.

Based on EHI, SRH and BRN analyses of difference of TOPOM100 from TOPOM0 simulations, regarding the importance of complex terrain, T07 was followed by T10. The least affection of topography was recorded during T11 event, for EHI, SRH and BRN diagnostic variables. MCAPE analyses of difference of TOPOM100 from TOPOM0 simulations, revealed that topography played an important factor for T07 event. During T10 event complex terrain played a positive factor only 20 min prior to tornado development. Simulation with TOPOM100 at T11 event revealed that MCAPE values were significant higher than TOPOM0 run.

At T07 event, topography revealed that it was an important factor for all diagnostic variables, as all values of TOPOM0 were actually double compared with TOPM100 simulation. During T07 event the storm propagated E-NE, over a steep slope terrain, from the coast of Corinthian's Gulf to a complex terrain of 1200 m elevation. EHI, MCAPE and SRH variable showed a significant increase 30 min prior of T07 tornado event.

7 Summary and conclusions

Three tornado events that occurred over the last years in Greece have been selected for numerical experiments in order to investigate the role of topography in significant tornado-genesis events that were triggered under strong synoptic scale forcing. The first tornado event (T07) occurred in Thiva (Boeotia, on 17 November 2007), the second event (T10) in Vrastema (Chalkidiki, on 12 February 2010) and the last one (T11) in Vlychos (Lefkada, on 20 September 2011). These events were associated with synoptic scale forcing, while their intensity was T4–T5 (Torro scale) and caused significant damage.

Numerical simulations were performed using the non-hydrostatic Weather Research and Forecasting (WRF, ARW core) model. Three one-way nested domains were utilised with spatial resolution of 12 km for D1, 4 km for D2 and 1.333 km for D3 domain. Initialised and lateral boundary conditions for the D1 domain were obtained from ECMWF ERA-Interim dataset, with ECMWF gridded analyses, with telescoping nested grids that allow the representation of atmospheric circulations ranging from the synoptic scale down to the meso scale. WRF-ARW model parameterization setup was able to forecast in a lead time of more than 12 h significant values of diagnostic variables.In the experiments the topography of the inner grid (D3) was modified by: (a) 0 % (actual topography) and (b) −100 % (without topography). Analyses concern a dataset of diagnostic instability variables: EHI, BRN, SRH and MCAPE.

According the model verification in this study, the model errors are generally within the values that appear in the literature, with a few exceptions (e.g. the 2 m temperature

NHESSD
2, 1433–1464, 2014

at LGTS, the 2 m dew-point temperature at LGPZ). The analysis of absolute vorticity budget revealed that in all cases the simulations with topography are associated with higher values of maximum absolute vorticity in the area of interest than those without topography. Similarly, the vorticity equation terms that determine the Eulerian time change of vorticity display higher maximum values in the experiment with topography. The differences between the two experiments, and the concomitant importance of topography for tornado genesis, are more distinguishable in the cases of 17 November 2007 and 12 February 2010. The similar values of maximum absolute vorticity and maximum vorticity equation terms in the two experiments of T11 event, suggest that in this case the topography played a minor role and the synoptic forcing dominated.

Numerical simulations revealed that the complex topography was denoted as an important factor during 17 November 2007, 12 February 2010 events, based on EHI and BRN analyses. Topography around 20 September 2011 event was characterized as the least factor based on EHI, SRH, BRN analyses.

Considering the time of tornadoes' occurrence and MSL synoptic analysis charts, from UK Met Office (UKMO), all tornadoes were formed within storms that were associated with a synoptic force ingredient. All events occurred in the pro-frontal activity area, ahead of cold front.

Acknowledgements. The authors thank the Hellenic National Meteorological Service (HNMS) for providing all the necessary graphics and remote sensor dataset, associated with the tornadic events. The European Centre for Medium-range Weather Forecasts (ECMWF) is thanked for providing the data used to generate the initial and boundary conditions for the WRF-ARW runs. Authors acknowledge UK MetOffice (UKMO) and the http://www.wetter3.de for giving the ability to retrieve the UKMO's MSL pressure analysis charts.

NHESSD
2, 1433–1464, 2014

References

Basiakos, I., Katsaras, P., Alexiou, I., Mavroudis, A., Karanikas, T., and Skrimizeas, P.: Operational Workstations at the Hellenic National Meteorological Service & a Windows NT Based Briefing System, 11th European Working Group on Operational Meteorological Workstations (11th EGOWS), 5–8 June 2000, Helsinki, Finland, 2000.

Bosart, L. F., Seimon, A., LaPenta, K. D., and Dickinson, M. J.: Supercell tornadogenesis over complex terrain: the Great Barrington, Massachusetts, tornado on 29 May 1995, Weather Forecast., 21, 897–922, 2006.

Braun, S. A. and Monteverdi, J. P.: An analysis of a mesocyclone-induced tornado occurrence in Northern California, Weather Forecast., 6, 13–31, 1991.

Brooks, H. E.: Proximity soundings for severe convection for Europe and the United States from reanalysis data, Atmos. Res., 93, 546–553, 2009.

Brooks, H. E., Doswell III, C. A., and Kay, M. P.: Climatological estimates of local daily tornado probability for the United States, Weather Forecast., 18, 626–640, 2003.

Chen, F. and Dudhia, J.: Coupling an advanced land-surface/hydrology model with the Penn State/NCAR MM5 modeling system, Part I: Model description and implementation, Mon. Weather Rev., 129, 569–585, 2001.

Craven, J. P. and Brooks, H. E.: Baseline climatology of sounding derived parameters associated with deep, moist convection, Preprints, 21st Conference on Severe Local Storms, 12–16 August 2002, St. Antonio, TX, USA, 2002.

Davies-Jones, R. D., Burgess, and Foster, M.: Test of helicity as a tornado forecast parameter, Preprints, 16th Conf. on Severe Local Storms, Kananaskis Park, AB, Canada, Amer. Meteor. Soc., 588–592, 1990.

Dee, D. P., Uppala, S. M., Simmons, A. J., Berrisford, P., Poli, P., Kobayashi, S., Andrae, U., Balmaseda, M. A., Balsamo, G., Bauer, P., Bechtold, P., Beljaars, A. C. M., van de Berg, L., Bidlot, J., Bormann, N., Delsol, C., Dragani, R., Fuentes, M., Geer, A. J., Haimberger, L., Healy, S. B., Hersbach, H., Hólm, E. V., Isaksen, L., Kållberg, P., Köhler, M., Matricardi, M., McNally, A. P., Monge-Sanz, B. M., Morcrette, J. J., Park, B. K., Peubey, C., de Rosnay, P., Tavolato, C., Thépaut, J. N., and Vitart, F.: The ERA-Interim reanalysis: configuration and performance of the data assimilation system, Q. J. Roy. Meteor. Soc., 137, 553–597, doi:10.1002/qj.828, 2011.

NHESSD
2, 1433–1464, 2014

Doswell III, C. A.: The distinction between large-scale and mesoscale contribution to severe convection: a case study example, Weather Forecast., 2, 3–16, 1987.
Doswell III, C. A. and Evans, J. S.: Proximity sounding analysis for derechos and supercells: an assessment of similarities and differences, Atmos. Res., 67–68, 117–133, 2003.
Doswell III, C. A. and Schultz, D. M.: On the use of indices and parameters in forecasting severe storms, Electronic J. Severe Storms Meteor., 1, 1–22, 2006.
Doswell III, C. A., Brooks, H. E., and Maddox, R. A.: Flash flood forecasting: an ingredients-based methodology, Weather Forecast., 11, 560–580, 1996.
Droegemeier, K. K., Lazarus, S. M., and Davies-Jones, R. D.: The influence of helicity on numerically simulated convective storms, Mon. Weather Rev., 121, 2005–2029, 1993.
Ebert, E. E.: Fuzzy verification of high-resolution gridded forecasts: a review and proposed framework, Meteorol. Appl., 15, 51–64, 2008.
Ferrier, B., Lin, Y., Black, T., Rogers, E., DiMego, G.: Implementation of a new grid-scale cloud and precipitation scheme in the NCEP Eta model, Prepr, 15th Conference on Numerical Weather Prediction, San Antonio, TX, Am. Meteorol. Soc., 280–283, 2002.
Glickman, T. S.: Glossary of Meteorology, 2nd edn., Am. Meteor. Soc.„ 855 pp., 2000.
Gofa, F., Pytharoulis, I., Andreadis, T., Papageorgiou, I., Fragkouli, P., Louka, P., Evgoustoglou, E., and Tyrli, V.: Evaluation of the operational NWP forecasts of the Hellenic National Meteorological Service, 9th Conference on Meteorology, Climatology and Atmospheric Physics, 28–31 May 2008, Thessaloniki, 51–58, 2008.
Groenemeijer, P. and van Delden, A.: Sounding-derived parameters in the vicinity of large hail and tornadoes in the Netherlands, Atmos. Res., 67, 273–299, 2007.
Groenemeijer, P., Corsmeier, U., and Kottmeier, Ch.: The development of tornadic storms on the cold side of a front favoured by local enhancement of moisture and CAPE, Atmos. Res., 100, 765–781, 2011.
Hannesen, R., Dotzek, N., Gysi, H., and Beheng, K. D.: Case study of a tornado in the Upper Rhine valley, Meteorol. Z., 7, 163–170, 1998.
Hart, J. A. and W. Korotky, W.: The SHARP Workstation v1.50 Users Guide, National Weather Service, NOAA, US Department of Commerce, 30 pp., 1991.
Houze Jr, R. A.: Cloud Dynamics, Academic Press Inc., San Diego, California, 1993.
Homar, V., Gaya, M., Romero, R., Ramis, C., and Alonso, S.: Tornadoes over complex terrain: an analysis of the 28th August 1999 tornadic event in eastern Spain, Atmos. Res., 67, 301–317, 2003.

NHESSD
2, 1433–1464, 2014

Effect of Greek complex topography on tornado genesis

I. T. Matsangouras et al.

Iacono, M. J., Delamere, J. S., Mlawer, E. J., Shephard, M. W., Clough, S. A., and Collins, W. D.: Radiative forcing by long-lived greenhouse gases: calculations with the AER radiative transfer models, J. Geophys. Res., 113, D13103, doi:10.1029/2008JD009944, 2008.

Janjic, Z. I.: The surface layer in the NCEP Eta Model, Eleventh Conference on Numerical Weather Prediction, 19–23 August 1996, Amer. Meteor. Soc., Norfolk, VA, 354–355, 1996.

Janjic, Z. I.: Nonsingular Implementation of the Mellor–Yamada Level 2.5 Scheme in the NCEP Meso model, NCEP Office Note, No. 437, 61 pp., 2002.

Johns, R. H. and Doswell III, C. A.: Severe local storms forecasting, Weather Forecast., 7, 588–612, 1992.

Johns, R. H., Davies, M., and Leftwich, P. M.: Some wind and instability parameters associated with strong and violent tornadoes, Part II: Variations in the combinations of wind and instability parameters, in: The Tornado: Its Structure, Dynamics, Hazards, and Prediction, Geophys. Monogr., Vol. 79, Amer. Geophys. Union, 583–590, 1993.

Kain, J. S.: The Kain–Fritsch convective parameterization: an update, J. Appl. Meteorol., 43, 170–181, 2004.

Matsangouras, I. T. and Nastos, P. T.: The 27 July 2002 tornado event in Athens, Greece, Adv. Sci. Res., 4, 9–13, 2010.

Matsangouras, I. T., Nastos, P. T., and Nikolakis, D.: Study of meteorological conditions related to the tornado activity on 25 March 2009 over NW Peloponnesus, Greece, in: Proc. 10th International Conference on Meteorology, Climatology and Atmospheric Physics (COMECAP2010), 25–38 May 2010, Patras, Greece, 417–425, 2010 (in Greek).

Matsangouras, I. T., Nastos, P. T., and Pytharoulis, I.: Synoptic-mesoscale analysis and numerical modelling of a tornado event on 12 February 2010 in northern Greece, Adv. Sci. Res., 6, 187–194, 2011a.

Matsangouras, I. T., Nastos, P. T., and Sioutas, M. V.: 300 years historical records of tornadoes, waterspouts and funnel clouds over Greece, 6th European Conference on Severe Storms (ECSS 2011), Palma de Mallorca, Balearic Islands, Spain, 3–7 October 2011, ECSS2011-215, 2011b.

Matsangouras, I. T., Nastos, P. T., and Pytharoulis, I.: Numerical investigation of the role of topography in tornado events in Greece, in: Advances in Meteorology, Climatology and Atmospheric Physics , edited by: Helmis, C. G. and Nastos, P. T., Springer, Berlin, Heidelberg, 209–215, doi:10.1007/978-3-642-29172-2_30, 2012.

NHESSD
2, 1433–1464, 2014

Effect of Greek complex topography on tornado genesis

I. T. Matsangouras et al.

Matsangouras, I. T., Nastos, P. T., Bluestein, H. B., and Sioutas, M. V.: A climatology of tornadic activity over Greece based on historical records, Int. J. Climatol., in press, doi:10.1002/joc.3857, 2013.
Meaden, G.: Tornadoes in Britain: their intensities and distribution in space and time, J. Meteorol., 1, 242–251, 1976.
Mellor, G. L. and Yamada, T.: Development of a turbulence closure model for geophysical fluid problems, Rev. Geophys. Space Ge., 20, 851–875, 1982.
Miglietta, M. M. and Regano, A.: An observational and numerical study of a flash-flood event over south-eastern Italy, Nat. Hazards Earth Syst. Sci., 8, 1417–1430, doi:10.5194/nhess-8-1417-2008, 2008.
Moncrieff, M. W. and Green, J. S. A.: The propagation and transfer properties of steady convective overturning in shear, Q. J. Roy. Meteor. Soc., 98, 336–352, 1972.
Monteverdi, J. P., Doswell III, C. A., and Lipari, G. S.: Shear parameter thresholds for forecasting tornadic thunderstorms in northern and central California, Weather Forecast., 18, 357–370, 2003.
Nastos, P. T. and Matsangouras, J. T.: Tornado activity in Greece within the 20th century, Adv. Geosci., 26, 49–51, doi:10.5194/adgeo-26-49-2010, 2010.
Nastos, P. T. and Matsangouras, I. T.: Composite mean and anomaly of synoptic conditions for tornadic days over North Ionian Sea (NW Greece), in: Advances in Meteorology, Climatology and Atmospheric Physics, edited by: Helmis, C. G. and Nastos, P. T., Springer, Berlin, Heidelberg, 639–645, doi:10.1007/978-3-642-29172-2_91, 2012.
Papadopoulos, A. and Katsafados, P.: Verification of operational weather forecasts from the POSEIDON system across the Eastern Mediterranean, Nat. Hazards Earth Syst. Sci., 9, 1299–1306, doi:10.5194/nhess-9-1299-2009, 2009.
Pytharoulis, I.: High-resolution operational numerical weather forecasts for agrometeorological applications, in: 6th Hellenic Conference of Agricultural Engineering, 8–10 October 2009, Thessaloniki, Greece, 75–82, 2009 (in Greek).
Rasmussen, E. N.: Refined supercell and tornado forecast parameters, Weather Forecast., 18, 530–535, 2003.
Rasmussen, E. N. and Blanchard, D. O.: A baseline climatology of sounding-derived super-cell and tornado forecast parameters, Weather Forecast., 13, 1148–1164, 1998.
Schaefer, J. T.: Severe thunderstorm fore-casting: a historical perspective, Weather Forecast., 1, 164–189, 1986.

Sioutas, M. V.: A tornado and waterspout climatology for Greece, Atmos. Res., 100, 344–356, 2011.
Sioutas, M. V., Nastos, P. T., Matsangouras, I. T., and Floca, H. A.: Meteorological conditions associated with strong tornadoes in Greece, in: Advances in Meteorology, Climatology and Atmospheric Physics, edited by: Helmis, C. G. and Nastos, P. T., Springer, Berlin, Heidelberg, 293–299, doi:10.1007/978-3-642-29172-2_42, 2012.
Thompson, R. L., Edwards, R., Hart, J. A., Elmore, K. L., and Markowski, P.: Close proximity soundings within supercell environments obtained from the Rapid Update Cycle, Weather Forecast., 18, 1243–1261, 2003.
Skamarock, W. C., Klemp, J. B., Dudhia, J., Gill, D. O., Barker, D. M., Duda, M. G., Huang, X.-Y., Wang, W., and Powers, J. G.: A Description of the Advanced Research WRF Version 3.NCAR/TN-475, 2008.
Wang, W., Bruyere, C., Duda, M., Dudhia, J., Gill, D., Lin, H.-C., Michalakes, J., Rizvi, S., Zhang, X., Beezley, J., Coen, J., and Mandel, J.: ARW Version 3 Modeling System User's Guide, NCAR-MMM, 352 pp., 2010.
Weisman, M. L. and Klemp, J. B.: The dependence of numerically simulated convective storms on vertical wind shear and buoyancy, Mon. Weather Rev., 110, 504–520, 1982.
Weisman, M. L. and Klemp, J. B.: The structure and classification of numerically simulated convective storms in directionally varying wind shear, Mon. Weather Rev., 112, 2479–2498, 1984.

NHESSD
2, 1433–1464, 2014

Effect of Greek complex topography on tornado genesis

I. T. Matsangouras et al.

Table 1. A selection of indices commonly used for severe storm forecasting. In the formulae, T denotes a temperature and D denotes a dew point temperature in °C, with a subscript indicating at what mandatory pressure level (in hPa) this value is to be taken from; α denotes the specific volume and a subscript lp denotes a value associated with a lifted parcel; LFC stands for a lifted parcel's level of free convection and EL stands for its equilibrium level. For the Bulk Richardson number, U_0 denotes the density weighted speed of the mean vector wind in the layer 0–6 km, and U denotes the speed of the mean vector wind in the layer from the surface to 500 m – the quantity is some-times referred to as the "BRN shear". For the storm-relative helicity, C denotes the storm motion vector.

Index Name	Formula	Reference
Convective Potential Available Energy (CAPE)	$\mathrm{CAPE} = \int_{\mathrm{LFC}}^{\mathrm{EL}} (\alpha_{lp} - \alpha)\mathrm{d}p$	Glickman (2000, p. 176)
Bulk Richardson Number (BRN)	$\mathrm{BRN} = \frac{\mathrm{CAPE}}{\frac{1}{2}(\overline{U} - U_0)^2}$	Weisman and Klemp (1982)
Storm Relative Helicity (SRH)	$\mathrm{SRH} = -\int_{z}^{z_0} k \left[(V_h - c)x\frac{\partial V_h}{\partial_z} \right] \mathrm{d}z$	Davies-Jones et al. (1990)
Energy Helicity Index (EHI)	$\mathrm{EHI} = \frac{(\mathrm{CAPE})(\mathrm{SRH})}{160\,000}$	Hart and Korotky (1991)

NHESSD
2, 1433–1464, 2014

Table 2. Statistical measures of 10 m wind speed (WS), temperature (T), dew point temperature (Td) and mean sea-level pressure (MSLP) at the meteorological stations of the Hellenic National Meteorological Service at the airports of Tanagra (LGTG), Thessaloniki (LGTS), Cephalonia (LGKF) and Aktio (LGPZ). ME = Mean Error (WRF Simulated minus Observed value), MAE = Mean Absolute Error, RMSE = Root Mean Squared Error, Sample Size = number of valid pairs of simulated and observed values. The date of the model validation and the distance from the location of the corresponding tornado event are also indicated.

Date	17 Nov 2007	12 Feb 2010	20 Sep 2011	20 Sep 2011
Met. station	LGTG	LGTS	LGKF	LGPZ
Distance (km)	26	50	65	28
ME 10 m WS ($m s^{-1}$)	2.08	0.79	1.37	0.79
ME T (K)	3.36	0.59	1.84	2.06
ME Td (K)	0.89	0.17	2.94	3.35
ME MSLP (hPa)	−1.25	−2.06	0.33	−1.07
MAE 10 m WS ($m s^{-1}$)	3.07	1.78	1.95	3.32
MAE T (K)	4.41	1.73	1.94	3.16
MAE Td (K)	1.57	1.23	3.04	3.35
MAE MSLP (hPa)	1.28	2.08	1.20	2.05
RMSE 10 m WS ($m s^{-1}$)	3.71	2.33	2.47	4.05
RMSE T (K)	5.28	2.21	2.12	3.49
RMSE Td (K)	1.86	1.57	3.81	4.00
RMSE MSLP (hPa)	1.56	2.34	1.40	2.26
Sample size	21	48	29	39

NHESSD
2, 1433–1464, 2014

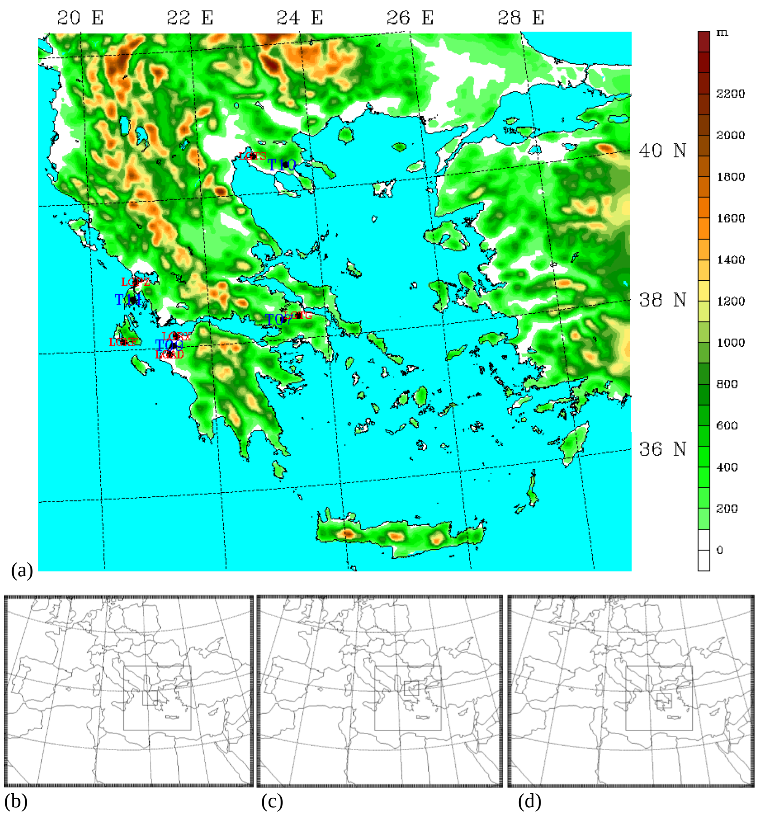

Fig. 1. The upper image **(a)** illustrates the actual topography of Greece with the location (black dots) of tornadoes and meteorological stations (blue and red abbreviations, respectively). The three nested domains used for numerical investigations of tornado events (lower images) are illustrated during **(b)** 17 November 2007, **(c)** 12 February 2010 and **(d)** 20 September 2011. In **(b)**, **(c)** and **(d)** images D1 is the outer domain, D3 is the inner domain and D2 is the intermediate domain.

NHESSD
2, 1433–1464, 2014

Fig. 2. Images **(a)** to **(h)** illustrate the impact of tornadoes to the local society: **(a)** and **(b)** in Thiva, on 17 November 2007 (source: courtesy of 1st author), **(c)** and **(d)** in Vrastama, on 12 February 2010 (source: http://forum.snowreport.gr/forumposts.asp?TID=23403\&PN=1), **(g)** and **(h)** in Vlychos, on 20 September 2011 (source: http://www.kolivas.de).

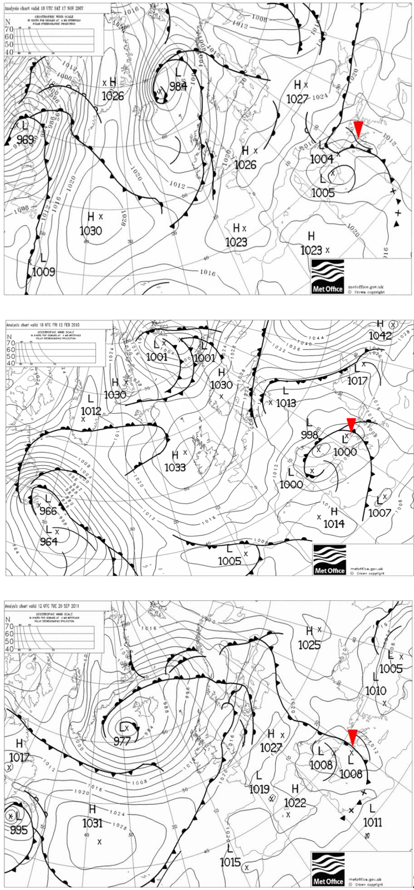

(a) 17 November 2007, 18:00 UTC

(b) 12 February 2010, 18:00 UTC

(c) 20 September 2011, 12:00 UTC

Fig. 3. MSL analysis charts, from UK Met Office, depicting the frontal activity, around tornadoes' time of occurrence for T07 **(a)**, T10 **(b)** and T11 **(c)** tornado events. Red arrow in every image indicates the tornado's location.

NHESSD

2, 1433–1464, 2014

Effect of Greek complex topography on tornado genesis

I. T. Matsangouras et al.

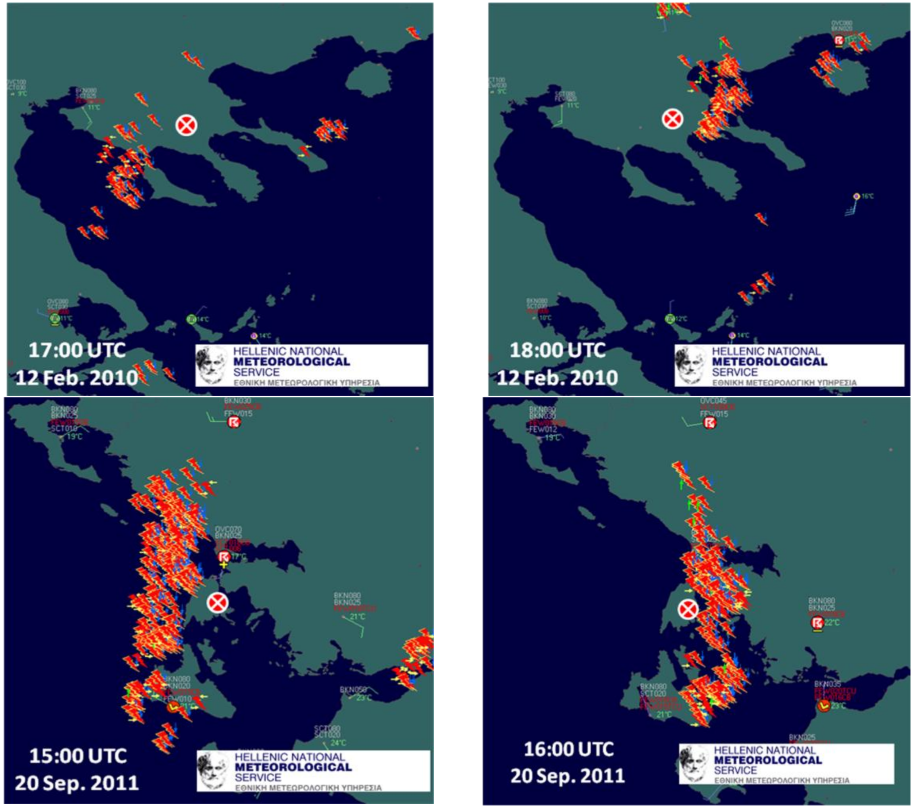

Fig. 4. Hourly visualization of weather conditions associated with T10 (upper images) and T11 (lower images) events. Tornadoes development within the above hourly time window and the white X in red circle denotes the location. Meteorological tactical reports (METAR) are plotted over the nearest weather stations; red symbols illustrate the spatial lightning activity.

a)
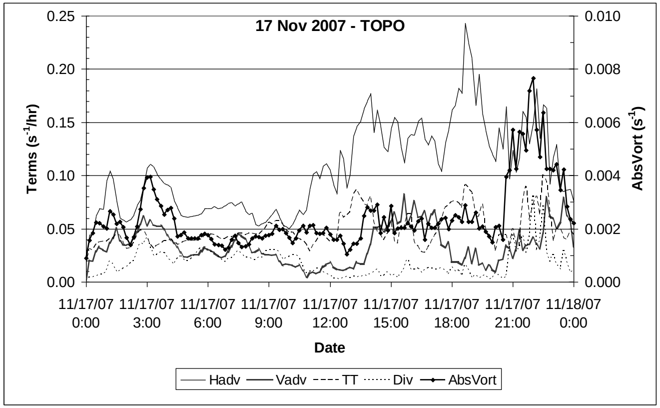

b)
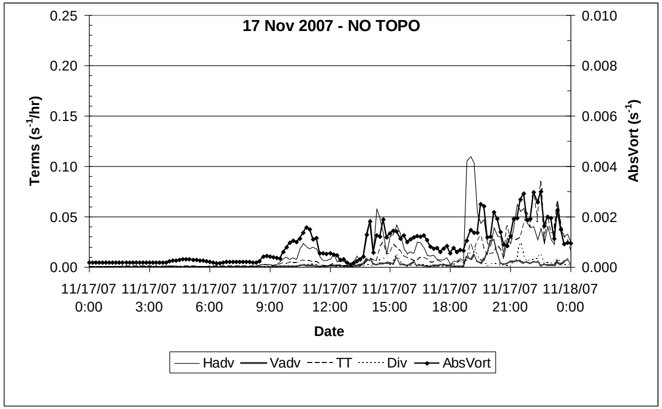

Fig. 5. Timeseries of WRF maximum simulated values of Absolute Vorticity (s^{-1}) and of the vorticity equation terms ($s^{-1}\,hr^{-1}$) of horizontal (Hadv) and vertical advection (Vadv), tilting/twisting (TT) and divergence (DIV), at 1 km above sea-level in a box of $0.2^{\circ} \times 0.2^{\circ}$ latitude-longitude centered at the actual location of the tornado of 17 November 2007. **(a)** with topography and **(b)** without topography.

NHESSD
2, 1433–1464, 2014

Effect of Greek complex topography on tornado genesis

I. T. Matsangouras et al.

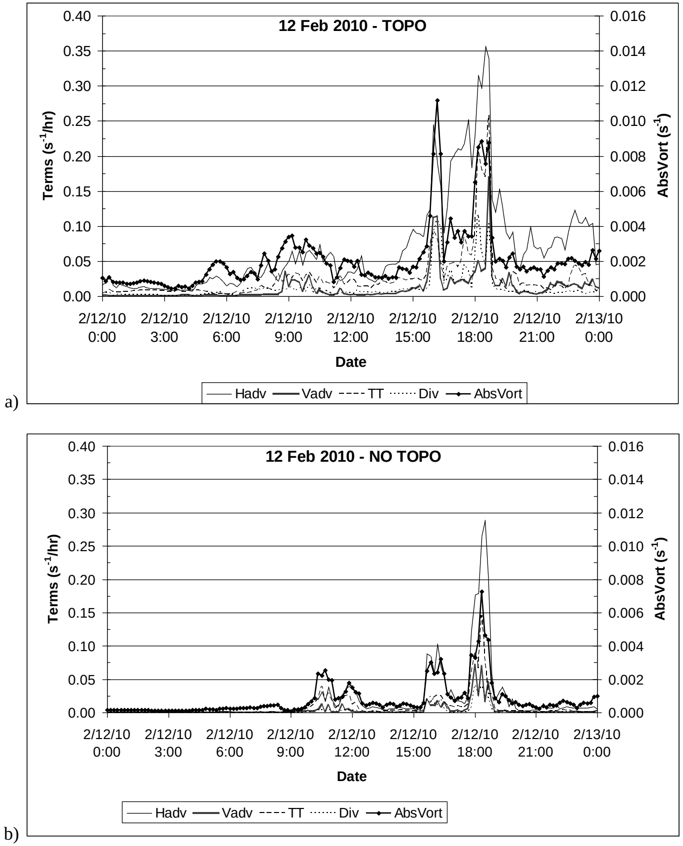

Fig. 6. Similar to Fig. 5 but for the case of 12 February 2010.

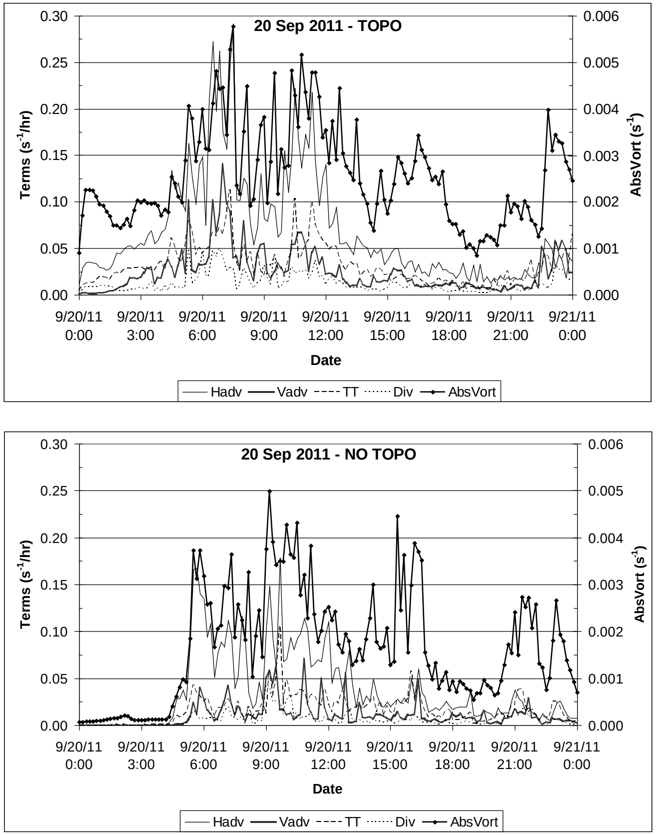

a)

b)

Fig. 7. Similar to Fig. 5 but for the case of 20 September 2011.

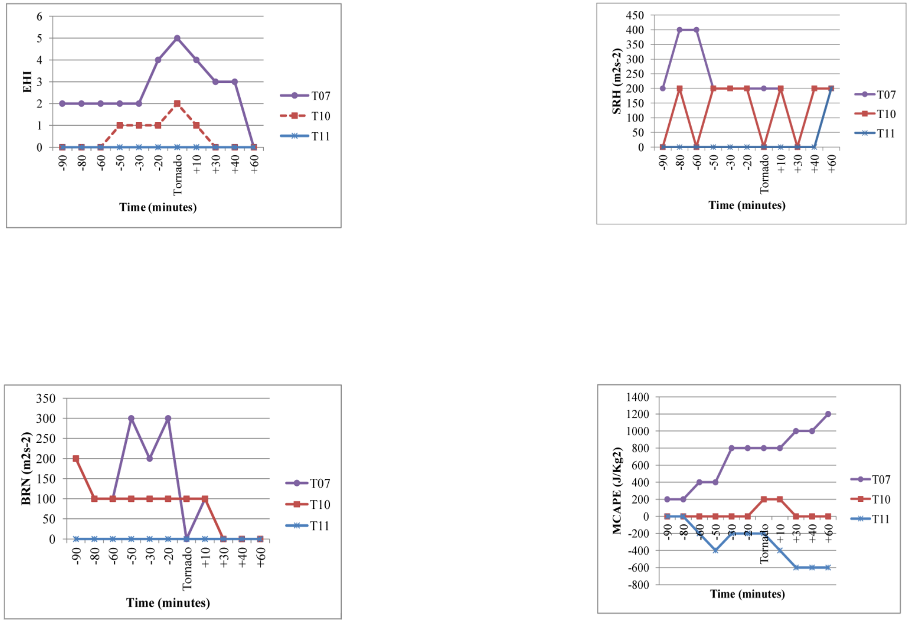

Fig. 8. Graphics illustrating the difference of TOPOM100 from TOPOM0 simulations (TOPOM0-TOPOM100) per diagnostic variable (EHI, SRH, BRN, and MCAPE) for every tornadic case study (T07, T10 and T11). Positive values implying a positive impact of topography, values equal to 0 implying no impact of topography and negative values implying a negative impact of topography to diagnostic variables.

NHESSD
2, 1433–1464, 2014